Journal of
Composites Science

MDPI

Article

Preparation and Characterization of SiO_2-PMMA and TiO_2-SiO_2-PMMA Composite Thick Films for Radiative Cooling Application

Dwi Fortuna Anjusa Putra , Uzma Qazi, Pin-Hsuan Chen and Shao-Ju Shih *

Department of Materials Science and Engineering, National Taiwan University of Science and Technology, No.43, Sec. 4, Keelung Road, Taipei 10607, Taiwan
* Correspondence: shao-ju.shih@mail.ntust.edu.tw; Tel.: +886-2-27303716

Abstract: Radiative cooling, an emerging technology that reflects sunlight and emits radiation into outer space, has gained much attention due to its energy-efficient nature and broad applicability in buildings, photovoltaic cells, and vehicles. This study focused on fabricating SiO_2-polymethyl methacrylate (PMMA) and TiO_2-SiO_2-PMMA thick films via the blade-coating method. The investigation aimed to improve cooling performance by adding TiO_2 particles to increase the coverage area and utilize the TiO_2 reflectance ability. The characterizations of the emissivity/absorptivity, solar reflectance, and microstructure of the thick films were conducted by using ultraviolet–visible/near-infrared (UV-Vis/NIR) diffuse reflection spectroscopy and scanning electron microscopy, respectively. Experimental results revealed that the maximum temperature drops of approximately 9.4 and 9.8 °C were achieved during the daytime period for SiO_2-PMMA and TiO_2-SiO_2-PMMA thick films. The total solar radiation reflectivity increased from 71.7 to 75.6% for SiO_2-PMMA radiative cooling thick films after adding TiO_2. These findings underscored the potential of TiO_2-SiO_2-PMMA thick films in advancing radiative cooling technology and cooling capabilities across various applications.

Keywords: radiative cooling; SiO_2; PMMA; TiO_2; blade coating

Citation: Putra, D.F.A.; Qazi, U.; Chen, P.-H.; Shih, S.-J. Preparation and Characterization of SiO_2-PMMA and TiO_2-SiO_2-PMMA Composite Thick Films for Radiative Cooling Application. *J. Compos. Sci.* **2024**, *8*, 453. https://doi.org/10.3390/jcs8110453

Academic Editor: Francesco Tornabene

Received: 29 August 2024
Revised: 19 October 2024
Accepted: 28 October 2024
Published: 1 November 2024

1. Introduction

The development of eco-friendly, non-energy-consuming materials is essential for reducing power consumption and mitigating the effects of global warming. Radiative cooling represents a passive and innovative approach that achieves temperature reduction without the need for energy input by emitting heat directly into outer space through the atmospheric window (8–13 μm) [1]. This process leverages the natural thermal radiation properties inherent in all objects, which govern the absorption and emission of heat energy [2]. By applying materials with selective radiation emission properties to surfaces, heat dissipation is optimized, ensuring that thermal radiation aligns with the atmospheric window's specific wavelengths. As a result, this technique effectively allows heat to escape into space, providing a sustainable means of cooling and contributing to the preservation of Earth's environment [3].

Numerous studies have focused on the high-emissivity materials in the atmospheric window, particularly silicon-based inorganic substances, including silicon monoxide (SiO) [4], silicon dioxide (SiO_2) [5,6], silicon carbide (SiC) [7], silicon nitride (Si_3N_4) [8], and silicon oxynitride (SiO_xN_Y) [9–11]. Among these materials, SiO_2 has been extensively studied and applied due to its superior optical properties, which makes it transparent to solar radiation, an ideal trait for solar radiation cooling [5,6]. Xiang, et al. tried to optimize SiO_2 film with three-dimensionally porous cellulose acetate (3-D PCA) to create pore sizes around ~5 μm. The film achieved solar reflectance of ~96% with an additional average infrared emittance of ~95%; further, the passive radiative cooling demonstrated could achieve a cooling temperature of ~8.6 °C (nighttime) and ~6.2 °C (daytime) based on morphology changed of SiO_2 could cause reflectance increment, especially in the atmospheric transmittance window [12]. SiO_2 exhibits increased extinction ratios at wavelengths of 10 and 20 μm, attributed to phonon polariton resonances [13]. However, the interface between bulk SiO_2 and air creates an impedance mismatch, raising reflectivity and reducing thermal radiation emission [14]. Consequently, research often employs SiO_2 films or nano- to submicron-scale SiO_2 particles to enhance thermal radiation emission through improved absorption and refraction [15].

Numerous researchers have shifted toward alternative cost-effective materials that can maintain or improve cooling performance. Materials such as titanium dioxide (TiO_2) [16–18], barium sulfate ($BaSO_4$) [19], and calcium carbonate ($CaCO_3$) [20] offer obvious advantages in this regard. For instance, studies have shown that replacing the expensive HfO_2 with TiO_2 in multilayer SiO_2 structures not only reduces costs but also enhances emission rates and cooling power [18]. These alternatives provide a more practical approach for large-scale applications, making radiative cooling technologies more accessible and economically viable. Based on the previous results, TiO_2 has been chosen most of the time due to its chemical stability, non-toxicity, availability, low cost, and minimal absorption in the visible optical region [21,22]. It also serves as an ultraviolet absorber in polymer coatings, extending their service life [23,24]. In other cases, studies have demonstrated that adding 0.1 and 0.6 μm TiO_2 particles improves solar radiation reflection [25,26]. For instance, Bao et al. [15] proposed a structure of double layers by adding the upper layer of TiO_2 particles as the reflective layer and the bottom layer with tightly stacked SiC or SiO_2 nanoparticles as the emission layer, sprayed on the aluminum plate (Al foil). The devices achieved reflectance in the solar spectrum of 90.70%, and in the emittance of the "sky window" reached 90.11% under drying conditions. As a result, a cooling effect of about °C lower than the ambient temperature in the sunshine was achieved, and the maximum temperature reduction in the substrate can be reduced to 8 °C under the sunshine conditions [15].

To solve the inherent brittleness, mechanical stability, and flexibility of the films, polymers are lightweight and easy to apply on large or complex surfaces, making them suitable for cooling automobiles, buildings, and solar photovoltaic cells. The polymers of polymethyl pentene [27], low-density polyethylene [16], acrylic resin [28,29], and polymethyl methacrylate (PMMA) [30,31] are commonly used as emitters due to their high visible light penetration. Among these polymers, PMMA was chosen in this study due to its excellent properties and high optical transparency in the visible and near-infrared regions. It could also withstand a wide range of temperatures without obvious degradation, ensuring the longevity of the cooling materials [16,30,31].

This study investigated the cooling capacities of SiO_2-PMMA and TiO_2-SiO_2-PMMA thick films by optimizing the preparation methods and adjusting powder addition ratios and thicknesses to enhance their daytime radiative cooling abilities. The phase compositions, morphologies, and optical properties were analyzed using X-ray diffraction (XRD), scanning electron microscopy (SEM), and ultraviolet–visible/near-infrared (UV-Vis/NIR) spectrophotometry. Finally, the individual performances of the radiative cooling films were evaluated through radiative cooling measurement.

2. Materials and Methods

2.1. Preparation of SiO_2-PMMA and TiO_2-SiO_2-PMMA Composite Thick Films

The radiative cooling film was fabricated using the common method of the blade-coating technique. The materials included 1 μm SiO_2 microsphere powder (Taiwan Union Abrasives Corp., Kaohsiung, Taiwan), silane-69 (Si-69) (Evermore Corp., Taipei, Taiwan), 2 μm PMMA balls (Aurora Applied Material Co., Ltd., Tainan, Taipei), and ~0.2 μm rutile TiO_2 particles (Chemours, Wilmington, DE, USA). SiO_2 solution and the polymer solution binder were prepared separately. For the SiO_2 solution, the preparation involved mixing silicon oxide microsphere powder (SiO_2, 1.39 g) as the template powder with Si-69 (silanol-69, 0.48 g) as a dispersant. Then, for the binder solution, a PMMA (1.15 g) with and without 5 vol% of TiO_2 in a 1,2-dichloroethane (1,2-DCE 99.5%, Fisher Chemical, Berlin, Germany) solution (15 mL) was prepared. Based on the previous study [32], the rutile phase exhibits a higher refractive index of 2.73 than that of the anatase phase (2.51) for TiO_2, which suggests that the rutile phase reflects more sunlight and has a better cooling performance than that of the anatase phase. Also, the 5 vol% of TiO_2 particles minimized the cracking of thick films by agglomeration of TiO_2 particles based on the previous reports of Cheng et al. [26] and Sun et al. [33]; therefore, the condition of adding 5 vol% of rutile TiO_2 particles was chosen in this study. This mixture was continuously stirred for 1 h, forming a turbid solution. A control solution without TiO_2 was also synthesized as a template film. Stainless steel (SS) 304 was chosen as the film substrate, and the thickness of the radiative cooling film was adjusted to approximately 80 µm. Each substrate was evenly coated and dried immediately without any additional heating. For testing the passive daytime radiative cooling (PDRC) film, a temperature data logger (model 88160, AZ Instrument Corp., Taichung, Taiwan) was employed alongside a custom-made chamber designed of about a 10 cm × 10 cm stainless steel 304 substrate coated using the blade-casting method. The insulation layer was dimensioned at 13 cm × 13 cm × 10 cm, with a chamber measuring volume of 10 cm × 10 cm × 4 cm (Figure 1a). Polystyrene was used to insulate and prevent external heat transfer, ensuring accurate measurement of the performance of PDRC films. The detailed design of the chamber is shown in Figure 1. To define the total percentage of each material on each film, a volume fraction (V_f) calculation has been carried out based on the equation of $V_f = V_{component}/V_{total}$.

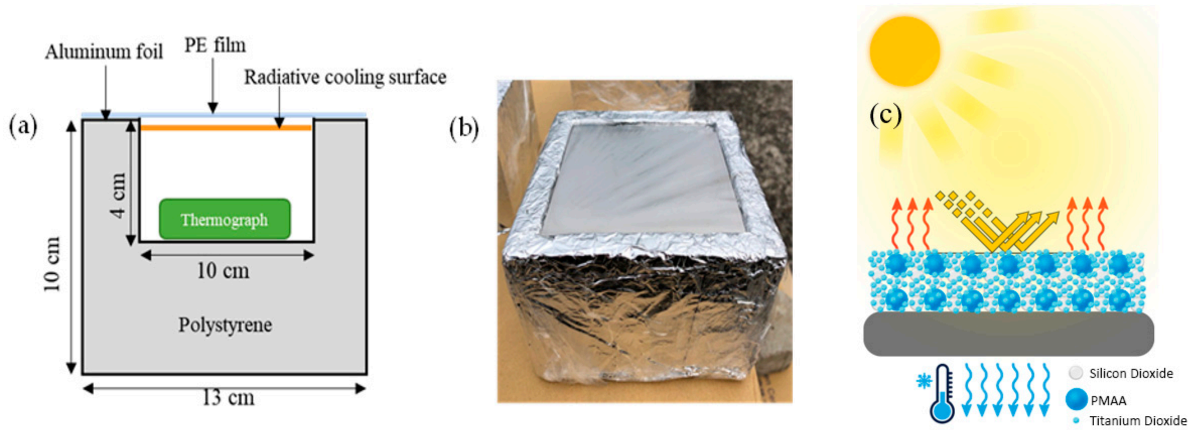

Figure 1. Temperature measurements of radiative cooling thick films: (**a**) cross-section schematic of the apparatus; (**b**) photograph of the on-site apparatus; (**c**) schematic figure of TiO_2-SiO_2-PMMA radiative cooling thick films (the red and blue arrows represent heat dissipation mechanisms).

The details of the volume fraction for all compositions in the thick films are shown in Table 1. Importantly, for measuring the performance of thick films, the diurnal data are shown, which include data for the relative humidity and temperature measurements taken from 10:00 a.m. to 6:00 p.m. on the assigned date.

Table 1. The volume fractions of composition for the radiative cooling thick films.

Sample Name	Composition (%)		
	TiO_2	SiO_2	PMMA
SiO_2-PMMA	-	35.0	65.0
TiO_2-SiO_2-PMMA	10.6	31.3	58.1

2.2. Structural Characterization

The phase compositions of the PDRC films were examined using an X-ray diffractometer (D2 Phaser, Bruker, Karlsruhe, Germany) equipped with a radiation lamp and a Ni filter. The scanning parameters included an increment of 0.05° per step and a scanning rate of 0.2°/s, covering a diffraction angle range from 20° to 80°. A field-emission scanning electron microscope (JSM 6500F, JEOL, Tokyo, Japan) was utilized in both back-scattering and secondary electron imaging modes to examine the surface morphologies of the films. Before observation, the films were coated with a thin layer of platinum using a sputter coater (E-1030, Hitachi, Tokyo, Japan). Measurements of the average particle sizes of powders were taken by sampling more than 100 particles with a couple of SEM images.

2.3. Optical Properties Characterization

The optical properties of the films were assessed using a UV-Vis/NIR spectrophotometer (Jasco V-670, Tokyo, Japan) covering the wavelength range from 50 to 2500 nm. This range was selected to cover the wavelength range of ultraviolet, visible light, and near-infrared spectra, ensuring a comprehensive analysis of the optical performance of the passive daytime radiative cooling film.

3. Results

This work focused on the precise control and optimization of the size distribution of SiO_2 and TiO_2 particles to maximize the cooling effect while minimizing UV absorption. Previous studies have discussed the advantages of mixed-sized particles or combining TiO_2 and SiO_2 for improving solar reflectance [26]. However, our research advances this by focusing on a synergistic design where the particle sizes are tailored to achieve optimal scattering across different solar spectrum regions. While previous research has utilized mixed-sized particles, our approach fine-tunes the particle size distribution of SiO_2 and TiO_2 specifically to enhance light scattering in both the visible and near-infrared regions, contributing to more effective radiative cooling. TiO_2 particles are used for visible light scattering, whereas larger SiO_2 particles help scatter near-infrared light without contributing to UV absorption. Meanwhile, the PMMA was used as a binder due to its better dispersion and distribution in composite materials [34], addressing the challenge of heating from UV absorption in $TiO_{2,}$ as illustrated in Figure 1c.

The SEM image of Figure 2 demonstrates a uniform distribution of spherical particles of SiO_2 with a relatively smooth surface morphology. The particles appear to have a narrow size distribution, with diameters predominantly in the sub-micron range around 1 ± 0.50 µm, similar to the product description (Figure 1a). On the other hand, the TiO_2 particles, as shown in Figure 2b, exhibit a more complex and agglomerated morphology than SiO_2. The particles are smaller, with diameters around the 0.26 ± 0.06 µm range. Lastly, the PMMA particles, depicted in Figure 2c, are larger and more irregular in shape compared to $SiO_{2,}$ with a particle size of around 1.5 ± 0.50 µm, which means the particle size was nearly double the particle size of SiO_2 particles. Based on the SEM observation, these particles have rougher surface textures, respectively.

The XRD patterns in Figure 3 reveal the structural intricacies and crystalline characteristics of the SiO_2-PMMA and TiO_2-SiO_2-PMMA thick films. For the SiO_2-PMMA thick film, the XRD pattern shows a broad hump around 20–30°, a hallmark of the amorphous nature of both SiO_2 and PMMA. On the other hand, the TiO_2-SiO_2-PMMA thick film displays sharp diffraction peaks, corresponding to the rutile phase of TiO_2, marked by a symbol (JCPDS number of 21-1276), indicating the TiO_2 on the rutile crystal structure. Based on the previous references [28,35], this is indicative of the refractive index of the rutile TiO_2 phase. As shown in Figure 3, the crystallite size of TiO_2 in the TiO_2-SiO_2-PMMA film is 0.27 ± 0.05 µm, calculated using the Scherrer equation.

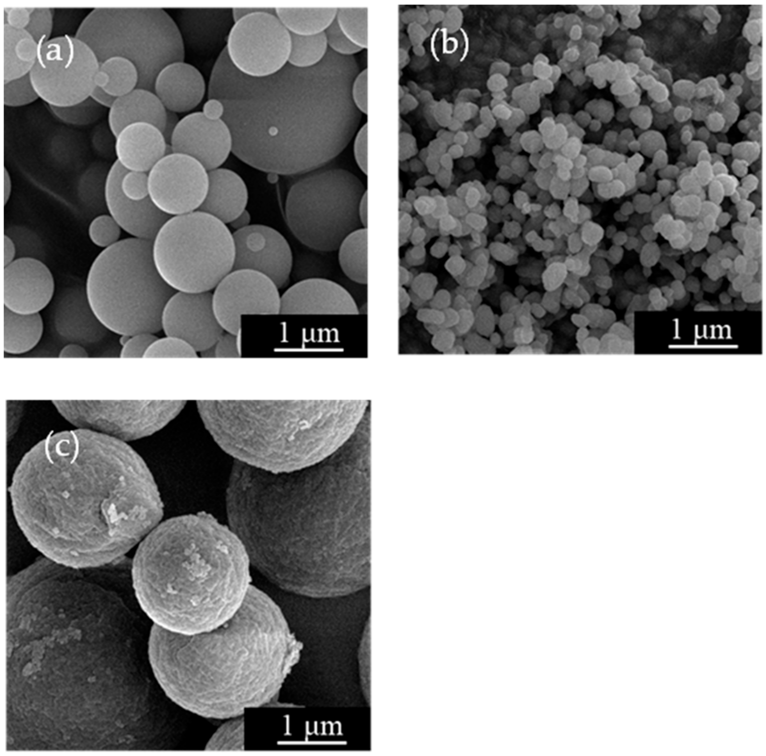

Figure 2. SEM images of (**a**) SiO_2, (**b**) TiO_2, and (**c**) PMMA particles.

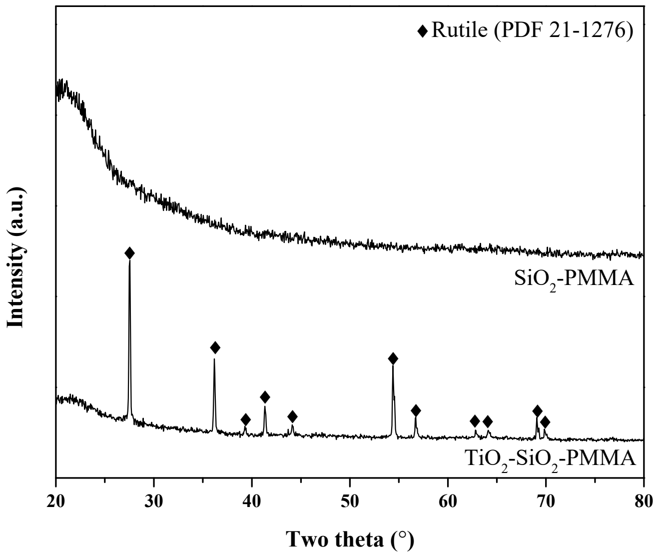

Figure 3. XRD patterns of SiO_2-PMMA and TiO_2-SiO_2-PMMA thick films.

Figure 4 presents secondary electron (SE) images of (a) SiO_2-PMMA and (b) TiO_2-SiO_2-PMMA thick films, each captured at a scale of 10 μm, highlighting their surface morphologies. The SiO_2-PMMA thick film reveals a densely packed arrangement of spherical SiO_2 particles within the PMMA matrix, ensuring high optical clarity and consistent light scattering essential for radiative cooling. In contrast, the TiO_2-SiO_2-PMMA thick film displays a more heterogeneous and textured surface due to incorporating TiO_2 particles, introducing additional roughness and complexity.

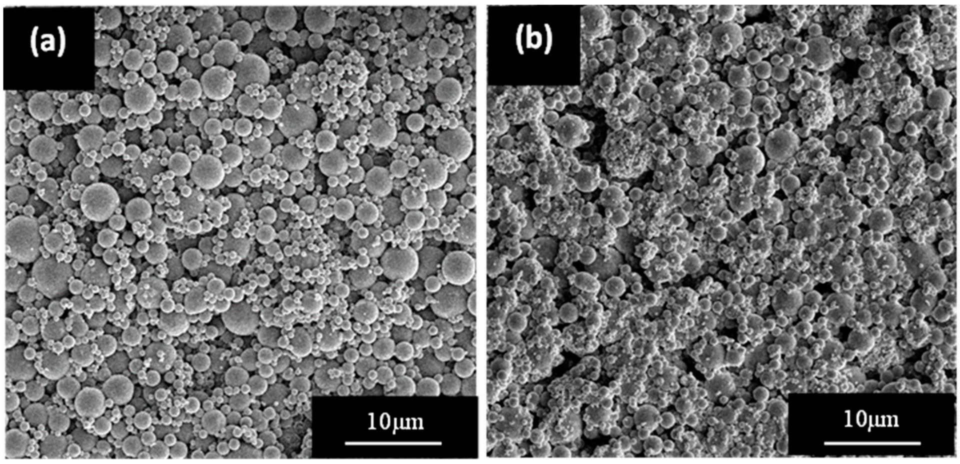

Figure 4. SE images of (**a**) SiO_2-PMMA and (**b**) TiO_2-SiO_2-PMMA thick films.

Figure 5 presents back-scattered electron (BSE) images of (a) SiO_2-PMMA and (b) TiO_2-SiO_2-PMMA thick films, with insets providing details on distinguishing every particle and higher magnification views at a scale of 2 μm. The SiO_2-PMMA thick film shows a uniform distribution of spherical SiO_2 particles within the PMMA matrix, with the inset revealing smooth and evenly sized particles, crucial for achieving high transparency and minimal light scattering. In contrast, the TiO_2-SiO_2-PMMA thick film features a more complex microstructure, with a denser packing of varying-sized particles and larger TiO_2 clusters surrounded by smaller SiO_2 particles. Due to its higher atomic number, the brighter appearance of TiO_2 in the BSE images underscores its obvious contribution to the composite's increased scattering and reflective properties [36,37].

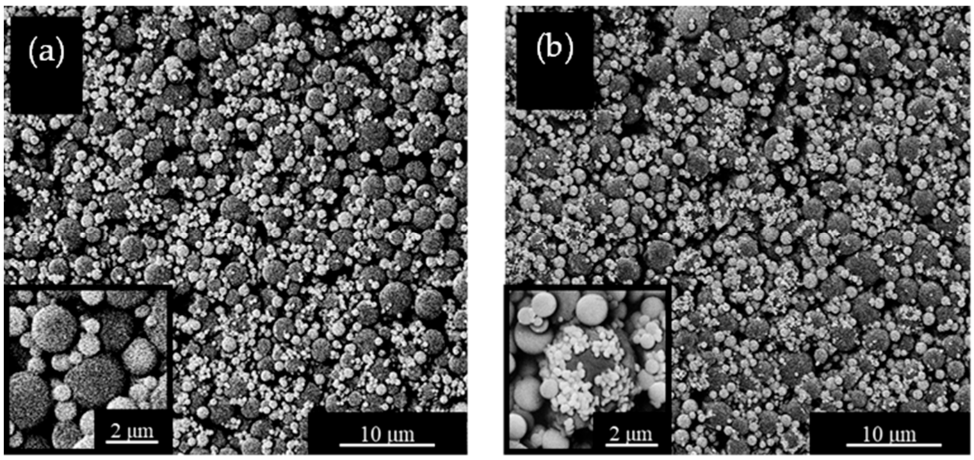

Figure 5. BSE images of (**a**) SiO_2-PMMA and (**b**) TiO_2-SiO_2-PMMA thick films.

Figure 6 shows the UV-Vis-NIR diffuse reflection spectrum. Since the coating with TiO_2 particles has a lower reflectance (higher absorption) in the UV–visible region (wavelength less than 410 nm), the reflectance is obviously higher than that of the coating without TiO_2 in a wavelength greater than 410 nm. To compare the solar reflectivity of each band, the solar reflectance of the coating layer in different bands was obtained by calculating the weighted average of the spectrum reflectance and the solar spectrum energy of AM1.5 (Table 2). The reflectance decreased from 42.3 to 14.1% in the ultraviolet region (UV), increased from 76.0 to 80.9% in the visible region (Vis), and increased from 70.2 to 75.4% in the near-red region (NIR). The total solar radiation reflectivity increased from 71.7 to 75.6%. However, the spectral reflectance of TiO_2 is not ideal in the ultraviolet region. The utilization of titanium dioxide (TiO_2) in coatings or films applied to polymer substrates has been the subject of extensive investigation in various studies. When exposed to prolonged ultraviolet (UV) light, polymer materials often deteriorate or age. However, the incorporation of TiO_2 emerges as a promising solution to this challenge. Through its ability to absorb UV light, TiO_2 effectively shields the coating layer from damage, enhancing overall reflectivity [26,38]. On the other hand, the infrared emissivity on the atmospheric window has been measured (Figure 7), and the total coverage area of 8–11 μm was conducted from 0.553 to 0.573 after adding the TiO_2, which did not give any obvious increase after adding TiO_2. Furthermore, TiO_2 acts as an ultraviolet absorbent, prolonging the object's service life and reducing deterioration or aging reactions [26]. In this experiment, the coating layer was not tested for aging. However, the reflectivity measurement proved that adding trace amounts of TiO_2 particles could increase the total reflectivity of the coating layer [26,38].

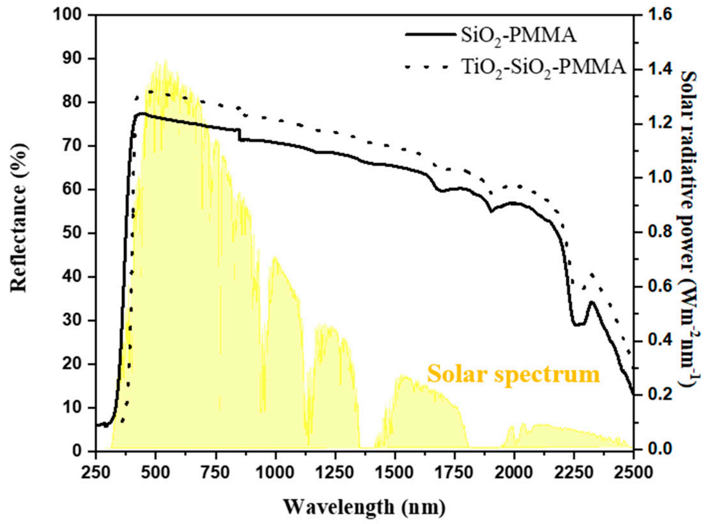

Figure 6. Reflectance of SiO_2-PMMA and TiO_2-SiO_2-PMMA thick films.

Table 2. The variation in the reflectance of the thick films with and without the incorporation of TiO_2 particles.

Sample Name	Solar Reflectance (%)		
	UV <410 nm	Vis 400~700 nm	NIR >700 nm
SiO_2-PMMA	42.3	76.0	70.2
TiO_2-SiO_2-PMMA	14.1	80.9	75.4

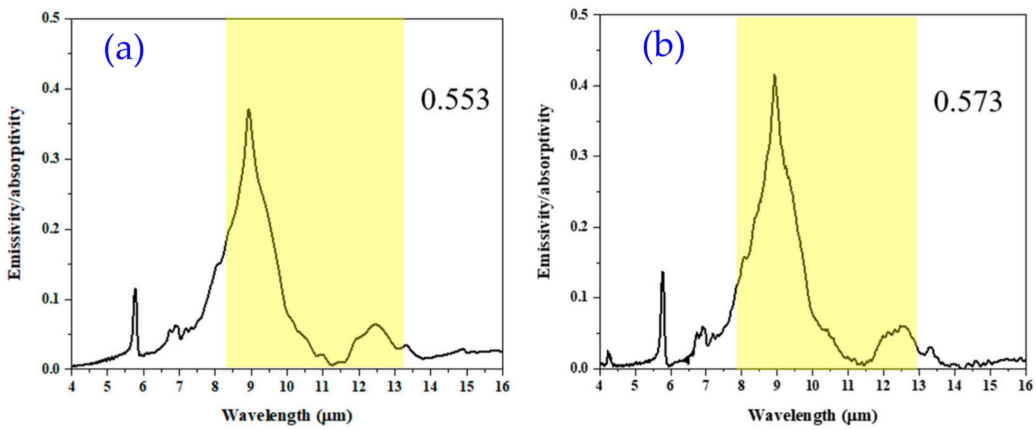

Figure 7. Infrared emissivity data of (**a**) SiO_2-PMMA and (**b**) TiO_2-SiO_2-PMMA thick films.

The graphs in Figure 8 illustrate the temperature profiles and temperature differences for substrates with and without the SiO_2-PMMA and TiO_2-SiO_2-PMMA thick films. In

Figure 8a, the black curve represents the temperature profile of the uncoated substrate, showing higher temperatures throughout the day, peaking above 55 °C under the camber. In contrast, the substrates coated with SiO_2-PMMA and TiO_2-SiO_2-PMMA exhibit lower temperatures, peaking just above 45 °C. The TiO_2-SiO_2-PMMA thick film shows a slightly better cooling performance than the SiO_2-PMMA thick film, maintaining a lower temperature throughout the day (the test was carried out in the summertime with a relative humidity (RH) of about 45–55% in the National Taiwan University of Science and Technology (NTUST) campus, Taiwan). Figure 8b highlights this cooling effect by depicting the temperature differences between the coated and uncoated substrates. Both coatings consistently reduce the substrate temperature by 8.0–9.8 °C, with the TiO_2-SiO_2-PMMA thick film offering a marginally more obvious reduction. These results underscore the effectiveness of the composite coatings in enhancing radiative cooling, with the TiO_2-SiO_2-PMMA thick film providing superior performance. This enhanced cooling capability is due to the synergistic combination of materials, which optimizes solar reflectance and thermal emissivity, making these coatings highly effective for passive radiative cooling applications.

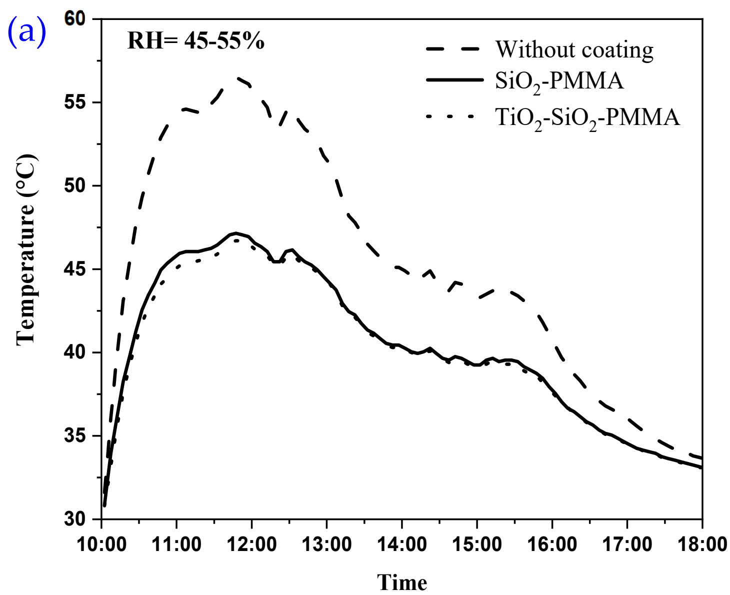

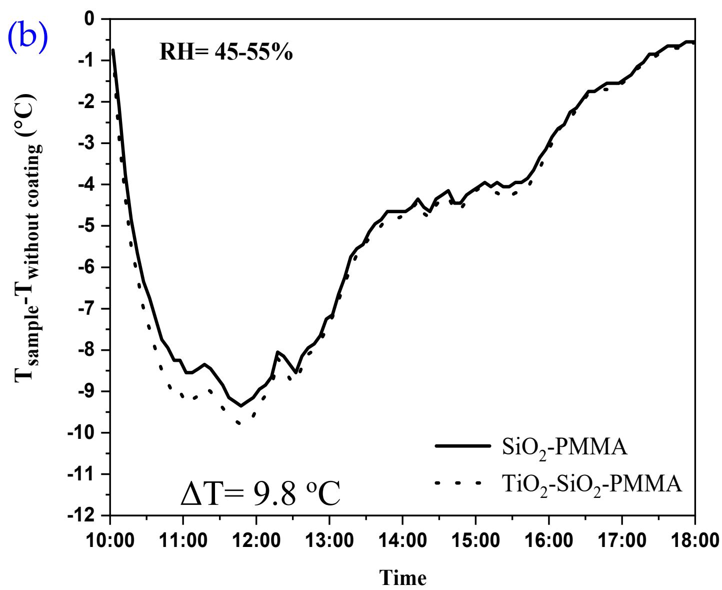

Figure 8. (**a**) Temperature profiles and (**b**) temperature difference of SiO_2-PMMA and TiO_2-SiO_2-PMMA thick films.

4. Discussion

The SEM image of SiO_2 particles demonstrates a uniform distribution of spherical particles with a relatively smooth surface morphology. However, the TiO_2 particles, as shown in Figure 2, exhibit a more complex and agglomerated morphology than SiO_2. The particles of TiO_2 are smaller and appear to form clusters or aggregates. This morphology is advantageous for radiative cooling because TiO_2 has a high covering area [39], enhancing the visible light's scattering. The agglomerated nature of TiO_2 particles can contribute to a broader scattering spectrum, thereby improving the cooling performance of the composite films when incorporated with other materials [26].

Based on the XRD data (see Figure 3), the amorphous SiO_2-PMMA and the crystalline TiO_2 within the TiO_2-SiO_2-PMMA thick film epitomizes an optimized composite structure. The amorphous SiO_2-PMMA matrix offers a firm film to the metal substrate, while the embedded rutile TiO_2 crystals enhance the optical and thermal properties due to their crystallinity [26]. This dual-phase integration is meticulously designed to maximize solar reflectance and thermal infrared emission, achieving superior passive cooling.

Figures 3 and 4 proved that the agglomeration of TiO_2 results in a highly covered area. The PMMA effectively attracts and binds TiO_2 particles to SiO_2, demonstrating its role as a successful binder. This morphology enhances the coverage, which is crucial for radiative cooling. According to references, the covering area impacts the efficiency of the radiative cooling mechanism. Evidence from the results and references indicates that adding rutile TiO_2 particles improves the reflectivity of the coating to solar radiation [38]. Based on the SE and BSE images of coatings with and without TiO_2 particles, the particle distribution in the coating reveals that TiO_2 particles coat the outer layer of PMMA particles, enhancing the overall performance of the coating. On the other hand, optimizing the particle size based on the cooling performance and optimizing particle size within a hierarchical structure can significantly enhance the cooling performance of radiative coatings. By carefully selecting and distributing particle sizes, we can maximize both light scattering and thermal emission, leading to more effective cooling solutions. Further experimental work and modeling will be crucial in developing coatings with tailored properties for specific applications [40–42].

This increased surface roughness enhances multi-angle light scattering and, combined with the high refractive index of TiO_2, improves solar reflectance and thermal emissivity [26,38]. These morphological differences underscore the tailored design of the TiO_2-SiO_2-PMMA composite thick film, optimizing it for superior radiative cooling performance. The synergistic effect of the amorphous SiO_2-PMMA matrix and crystalline TiO_2 particles makes the TiO_2-SiO_2-PMMA thick film an exemplary candidate for advanced passive cooling applications in various environmental conditions.

These factors could be a cause that progressively changes the reflectance and increases the UV absorbance of the SiO_2-PMMA obviously after TiO_2 doping [23]. The result could increase by about 12.5% compared to without TiO_2, and the obvious result is shown based on adding 5 vol% of TiO_2 (Figure 6). Meanwhile, the reflectance plays a role in comparing the emissivity at the atmospheric window region (as seen in Figure 7), revealing evidence that emissivity has a similar value for the thick film with and without TiO_2. The increasing reflectance of the radiative cooling film has been tested on the Daytime radiative cooling measurement, and the maximum temperature reduction could be achieved at 9.8 °C in the peak time on relatively high RH conditions and placed in the summertime of NTUST campus, Taiwan (Figure 8), respectively.

5. Conclusions

TiO_2-SiO_2-PMMA radiative cooling thick film was successfully fabricated and demonstrated an outstanding performance. We have collected information regarding the result. The TiO_2 in the SiO_2-PMMA matrix enhances the radiative cooling performance's thick film due to several key factors. SEM images reveal that TiO_2 particles, with a smaller diameter and more agglomerated morphology, provide a higher surface area and improved light scattering due to their high refractive index. XRD patterns show that the rutile phase of

TiO_2 introduces crystalline peaks due to the refractive index of rutile TiO_2, which would be beneficial for radiative cooling applications. The UV-Vis-NIR spectrum indicates that TiO_2 increases reflectance in the visible and near-infrared regions and UV absorbance. At the same time, SEM and BSE images demonstrate a more heterogeneous surface with TiO_2, improving overall light scattering. Temperature profiles reveal that TiO_2-SiO_2-PMMA thick film maintains lower temperatures throughout the day, reducing peak temperatures by approximately 9.8 °C compared to uncoated substrates. This superior cooling is attributed to the synergistic combination of materials, optimizing solar reflectance and thermal emissivity.

Author Contributions: Conceptualization, S.-J.S.; methodology, P.-H.C.; formal analysis, U.Q.; data curation, P.-H.C.; writing—original draft preparation, D.F.A.P.; writing—review and editing, D.F.A.P. and S.-J.S.; supervision, S.-J.S.; funding acquisition, S.-J.S. All authors have read and agreed to the published version of the manuscript.

Funding: The authors acknowledge the financial support from the National Science and Technology Council of Taiwan (grant number NSTC 111-2221-E-011-117-).

Data Availability Statement: The data presented in this study are available upon request from the corresponding author.

Conflicts of Interest: The authors declare no conflicts of interest.

References

1. Liu, M.; Zhang, S.; Li, F.; Zhang, C.; Zhu, H.; Wu, D. Performance of passive daytime radiative cooling coating with $CaSiO_3$ enhanced solar reflectivity and atmospheric window emissivity. *J. Phys. D Appl. Phys.* **2022**, *55*, 445501. [CrossRef]
2. Wijewardane, S.; Goswami, D. A review on surface control of thermal radiation by paints and coatings for new energy applications. *Renew. Sustain. Energy Rev.* **2012**, *16*, 1863–1873. [CrossRef]
3. Yang, J.; Zhang, X.; Zhang, X.; Wang, L.; Feng, W.; Li, Q. Beyond the visible: Bioinspired infrared adaptive materials. *Adv. Mater.* **2021**, *33*, 2004754. [CrossRef]
4. Granqvist, C.; Hjortsberg, A. Radiative cooling to low temperatures: General considerations and application to selectively emitting SiO films. *J. Appl. Phys.* **1981**, *52*, 4205–4220. [CrossRef]
5. Granqvist, C. Radiative heating and cooling with spectrally selective surfaces. *Appl. Opt.* **1981**, *20*, 2606–2615. [CrossRef] [PubMed]
6. Hjortsberg, A.; Granqvist, C. Infrared optical properties of silicon monoxide films. *Appl. Opt.* **1980**, *19*, 1694–1696. [CrossRef]
7. Zhao, B.; Hu, M.; Ao, X.; Chen, N.; Pei, G. Radiative cooling: A review of fundamentals, materials, applications, and prospects. *Appl. Energy* **2019**, *236*, 489–513. [CrossRef]
8. Hervé, A.; Drevillon, J.; Ezzahri, Y.; Joulain, K. Radiative cooling by tailoring surfaces with microstructures. *arXiv* **2018**, arXiv:1802.02067.
9. Sid-Ahmed, M.; Bilal, M.; Babiker, S. A Spectrally Selective Window for Hot Climates. *J. Electron. Cool. Therm. Control* **2017**, *7*, 2. [CrossRef]
10. Garg, H.; Dayal, M.; Furlan, G.; Sayigh, A.; Granqvist, C. Spectrally selective surfaces for heating and cooling applications. In *Physics and Technology of Solar Energy: Volume 2: Photovoltaic and Solar Energy Materials Proceedings of the International Workshop on Physics of Solar Energy, New Delhi, India, 24 November–6 December 1986*; Springer: Berlin/Heidelberg, Germany, 1987; pp. 191–276.
11. Eriksson, T.; Jiang, S.-J.; Granqvist, C. Surface coatings for radiative cooling applications: Silicon dioxide and silicon nitride made by reactive RF-sputtering. *Sol. Energy Mater.* **1985**, *12*, 319–325. [CrossRef]
12. Xiang, B.; Zhang, R.; Luo, Y.; Zhang, S.; Xu, L.; Min, H.; Tang, S.; Meng, X. 3D porous polymer film with designed pore architecture and auto-deposited SiO_2 for highly efficient passive radiative cooling. *Nano Energy* **2021**, *81*, 105600. [CrossRef]
13. Zhang, C.; Liao, W.; Zhang, L.; Jiang, X.; Chen, J.; Wang, H.; Luan, X.; Yuan, X. Large-area uniform periodic microstructures on fused silica induced by surface phonon polaritons and incident laser. *Opt. Lasers Eng.* **2018**, *105*, 101–105. [CrossRef]
14. Ding, Z.; Li, H.; Li, X.; Fan, X.; Jaramillo-Fernandez, J.; Pattelli, L.; Zhao, J.; Niu, S.; Li, Y.; Xu, H. Designer SiO_2 Metasurfaces for efficient passive radiative cooling. *Adv. Mater. Interfaces* **2024**, *11*, 2300603. [CrossRef]
15. Bao, H.; Yan, C.; Wang, B.; Fang, X.; Zhao, C.; Ruan, X. Double-layer nanoparticle-based coatings for efficient terrestrial radiative cooling. *Sol. Energy Mater. Sol. Cells* **2017**, *168*, 78–84. [CrossRef]
16. Raman, A.P.; Anoma, M.A.; Zhu, L.; Rephaeli, E.; Fan, S. Passive radiative cooling below ambient air temperature under direct sunlight. *Nature* **2014**, *515*, 540–544. [CrossRef] [PubMed]
17. Kecebas, M.A.; Menguc, M.P.; Kosar, A.; Sendur, K. Passive radiative cooling design with broadband optical thin-film filters. *J. Quant. Spectrosc. Radiat. Transf.* **2017**, *198*, 179–186. [CrossRef]
18. Jeong, S.Y.; Tso, C.Y.; Ha, J.; Wong, Y.M.; Chao, C.Y.; Huang, B.; Qiu, H. Field investigation of a photonic multi-layered TiO_2 passive radiative cooler in sub-tropical climate. *Renew. Energy* **2020**, *146*, 44–55. [CrossRef]

19. Li, X.; Peoples, J.; Yao, P.; Ruan, X. Ultrawhite $BaSO_4$ paints and films for remarkable daytime subambient radiative cooling. *ACS Appl. Mater. Interfaces* **2021**, *13*, 21733–21739. [CrossRef]
20. Lim, H.; Chae, D.; Son, S.; Ha, J.; Lee, H. $CaCO_3$ micro particle-based radiative cooling device without metal reflector for entire day. *Mater. Today Commun.* **2022**, *32*, 103990. [CrossRef]
21. Hashimoto, K.; Irie, H.; Fujishima, A. TiO_2 photocatalysis: A historical overview and future prospects. *Jpn. J. Appl. Phys.* **2005**, *44*, 8269. [CrossRef]
22. Berdahl, P.; Akbari, H.; Levinson, R.; Miller, W.A. Weathering of roofing materials—An overview. *Constr. Build. Mater.* **2008**, *22*, 423–433. [CrossRef]
23. Jaroenworaluck, A.; Sunsaneeyametha, W.; Kosachan, N.; Stevens, R. Characteristics of silica-coated TiO_2 and its UV absorption for sunscreen cosmetic applications. *Surf. Interface Anal.* **2006**, *38*, 473–477. [CrossRef]
24. Montazer, M.; Pakdel, E. Reducing photoyellowing of wool using nano TiO_2. *Photochem. Photobiol.* **2010**, *86*, 255–260. [CrossRef] [PubMed]
25. Peoples, J.; Li, X.; Lv, Y.; Qiu, J.; Huang, Z.; Ruan, X. A strategy of hierarchical particle sizes in nanoparticle composite for enhancing solar reflection. *Int. J. Heat Mass Transf.* **2019**, *131*, 487–494. [CrossRef]
26. Cheng, Z.; Shuai, Y.; Gong, D.; Wang, F.; Liang, H.; Li, G. Optical properties and cooling performance analyses of single-layer radiative cooling coating with mixture of TiO_2 particles and SiO_2 particles. *Sci. China Technol. Sci.* **2021**, *64*, 1017–1029. [CrossRef]
27. Zhai, Y.; Ma, Y.; David, S.N.; Zhao, D.; Lou, R.; Tan, G.; Yang, R.; Yin, X. Scalable-manufactured randomized glass-polymer hybrid metamaterial for daytime radiative cooling. *Science* **2017**, *355*, 1062–1066. [CrossRef]
28. Huang, Z.; Ruan, X. Nanoparticle embedded double-layer coating for daytime radiative cooling. *Int. J. Heat Mass Transf.* **2017**, *104*, 890–896. [CrossRef]
29. Ziming, C.; Fuqiang, W.; Dayang, G.; Huaxu, L.; Yong, S. Low-cost radiative cooling blade coating with ultrahigh visible light transmittance and emission within an "atmospheric window". *Sol. Energy Mater. Sol. Cells* **2020**, *213*, 110563. [CrossRef]
30. Zakharchenko, R.; Díaz-Flores, L.; Pérez-Robles, J.; González-Hernández, J.; Vorobiev, Y. Nanostructured porous sol-gel materials for applications in solar cells engineering. *Phys. Status Solidi* **2005**, *2*, 3308–3313. [CrossRef]
31. Palkovits, R.; Althues, H.; Rumplecker, A.; Tesche, B.; Dreier, A.; Holle, U.; Fink, G.; Cheng, C.; Shantz, D.; Kaskel, S. Polymerization of w/o microemulsions for the preparation of transparent SiO_2/PMMA nanocomposites. *Langmuir* **2005**, *21*, 6048–6053. [CrossRef]
32. O'Byrne, M.; Kerzabi, B.; Abbarchi, M.; Lifschitz, A.; Zamora, T.; Malgras, V.; Gourdin, A.; Modaresialam, M.; Grosso, D.; Putero, M. Investigation of the anatase-to-rutile transition for TiO_2 sol-gel coatings with refractive index up to 2.7. *Thin Solid Film.* **2024**, *790*, 140193. [CrossRef]
33. Sun, Y.; Javed, M.; Ji, Y.; Nawaz, M.Z.; Wang, Y.; Cai, Z.; Xu, B. Design and preparation of flexible double-layered daytime radiative cooling composite film with antifouling property. *Sol. Energy Mater. Sol. Cells* **2022**, *245*, 111836. [CrossRef]
34. Qi, G.; Tan, X.; Tu, Y.; Yang, X.; Qiao, Y.; Wang, Y.; Geng, J.; Yao, S.; Chen, X. Ordered-porous-array polymethyl methacrylate films for radiative cooling. *ACS Appl. Mater. Interfaces* **2022**, *14*, 31277–31284. [CrossRef] [PubMed]
35. Sun, J.; Wang, J.; Guo, T.; Bao, H.; Bai, S. Daytime passive radiative cooling materials based on disordered media: A review. *Sol. Energy Mater. Sol. Cells* **2022**, *236*, 111492. [CrossRef]
36. Lloyd, G.E. Atomic number and crystallographic contrast images with the SEM: A review of backscattered electron techniques. *Mineral. Mag.* **1987**, *51*, 3–19. [CrossRef]
37. Angker, L.; Nockolds, C.; Swain, M.V.; Kilpatrick, N. Quantitative analysis of the mineral content of sound and carious primary dentine using BSE imaging. *Arch. Oral Biol.* **2004**, *49*, 99–107. [CrossRef]
38. Wang, S.; Zhang, J. Effect of titanium dioxide (TiO_2) on largely improving solar reflectance and cooling property of high density polyethylene (HDPE) by influencing its crystallization behavior. *J. Alloys Compd.* **2014**, *617*, 163–169. [CrossRef]
39. Vilà, R.; Martorell, I.; Medrano, M.; Castell, A. Adaptive covers for combined radiative cooling and solar heating. A review of existing technology and materials. *Sol. Energy Mater. Sol. Cells* **2021**, *230*, 111275. [CrossRef]
40. Yu, Z.; Nie, X.; Yuksel, A.; Lee, J. Reflectivity of solid and hollow microsphere composites and the effects of uniform and varying diameters. *J. Appl. Phys.* **2020**, *128*, 053103. [CrossRef]
41. Atiganyanun, S.; Plumley, J.B.; Han, S.J.; Hsu, K.; Cytrynbaum, J.; Peng, T.L.; Han, S.M.; Han, S.E. Effective radiative cooling by paint-format microsphere-based photonic random media. *ACS Photonics* **2018**, *5*, 1181–1187. [CrossRef]
42. Atiganyanun, S. Use of hollow silica and titanium dioxide microparticles in solar reflective paints for daytime radiative cooling applications in a tropical region. *J. Photonics Energy* **2021**, *11*, 022103. [CrossRef]